OPEN

Journal of Cerebral Blood Flow & Metabolism (2015) 35, 1703–1710
© 2015 ISCBFM All rights reserved 0271-678X/15
www.jcbfm.com

ORIGINAL ARTICLE

# Positron emission tomography/magnetic resonance hybrid scanner imaging of cerebral blood flow using $^{15}$O-water positron emission tomography and arterial spin labeling magnetic resonance imaging in newborn piglets

Julie B Andersen[1], William S Henning[1], Ulrich Lindberg[2], Claes N Ladefoged[1], Liselotte Højgaard[1], Gorm Greisen[3] and Ian Law[1]

Abnormality in cerebral blood flow (CBF) distribution can lead to hypoxic–ischemic cerebral damage in newborn infants. The aim of the study was to investigate minimally invasive approaches to measure CBF by comparing simultaneous $^{15}$O-water positron emission tomography (PET) and single TI pulsed arterial spin labeling (ASL) magnetic resonance imaging (MR) on a hybrid PET/MR in seven newborn piglets. Positron emission tomography was performed with IV injections of 20 MBq and 100 MBq $^{15}$O-water to confirm CBF reliability at low activity. Cerebral blood flow was quantified using a one-tissue-compartment-model using two input functions: an arterial input function (AIF) or an image-derived input function (IDIF). The mean global CBF (95% CI) PET-AIF, PET-IDIF, and ASL at baseline were 27 (23; 32), 34 (31; 37), and 27 (22; 32) mL/100 g per minute, respectively. At acetazolamide stimulus, PET-AIF, PET-IDIF, and ASL were 64 (55; 74), 76 (70; 83) and 79 (67; 92) mL/100 g per minute, respectively. At baseline, differences between PET-AIF, PET-IDIF, and ASL were 22% ($P < 0.0001$) and − 0.7% ($P = 0.9$). At acetazolamide, differences between PET-AIF, PET-IDIF, and ASL were 19% ($P = 0.001$) and 24% ($P = 0.0003$). In conclusion, PET-IDIF overestimated CBF. Injected activity of 20 MBq $^{15}$O-water had acceptable concordance with 100 MBq, without compromising image quality. Single TI ASL was questionable for regional CBF measurements. Global ASL CBF and PET CBF were congruent during baseline but not during hyperperfusion.

*Journal of Cerebral Blood Flow & Metabolism* (2015) **35,** 1703–1710; doi:10.1038/jcbfm.2015.139; published online 10 June 2015

**Keywords:** $^{15}$O-water PET; arterial spin labeling; neonatology; PET; PET/MR

## INTRODUCTION

Abnormality in cerebral blood flow (CBF) distribution can lead to hypoxic–ischemic damage in newborn infants and is a major cause of later neurocognitive impairment.[1] Hypoxic–ischemic damage often occurs in the periventricular white matter of the preterm infant where CBF is low,[2,3] while regional hyperperfusion is associated with hypoxic–ischemic encephalopathy after asphyxia in term infants.[4–6] Thus, a clinically useful, robust, and accurate method for measuring CBF in newborn infants is needed.[7]

Monitoring of CBF in a region of the brain is possible by Doppler ultrasound and near infrared spectroscopy (NIRS), but these methods do not offer an imaging result. Imaging modalities of quantitative perfusion include single photon emission computed tomography, positron emission tomography (PET), and arterial spin labeling (ASL) magnetic resonance imaging (MR).

Positron emission tomography with $^{15}$O labeled water is considered the 'gold standard' in quantification of CBF[8,9] but the use is limited because of radiation exposure, limited access of the tracer, and need for laborious invasive procedures. In contrast, MR is broadly available, but the use of ASL in newborn infants is challenged by a number of factors that could impair the accuracy of the absolute values: low signal intensity because of the low blood content in the brain, limited water extraction in brain tissue, and inherent low CBF in newborn infants, all contributing to a low signal-to-noise ratio (SNR).

We have used our PET/MR system to compare quantitative global CBF values in newborn piglets with ASL and PET simultaneously, ensuring identical physiologic state and eliminating the disturbing effects because of unstable CBF. Furthermore, we tested the global CBF reliability of a low injected activity (20 MBq) of $^{15}$O-water and a minimally invasive image-derived input function (IDIF) from the left ventricle of the heart. The final aim was to develop a clinically useful method for imaging of CBF in newborn infants to later be able to study the pathophysiology of focal brain injury, such as stroke and periventricular leukomalacia.

## MATERIALS AND METHODS

The experimental protocol for the study was approved by the Danish Animal Experiments Inspectorate, license no. 2012-15-2934-00064 and conducted in accordance with the University of Copenhagen Animal Ethics Policy and with the ARRIVE (Animal Research: Reporting *In Vivo*

[1]Department of Clinical Physiology, Nuclear Medicine and PET, Rigshospitalet, University of Copenhagen, Copenhagen, Denmark; [2]Functional Imaging Unit, Glostrup Hospital, University of Copenhagen, Copenhagen, Denmark and [3]Department of Neonatology, Rigshospitalet, University of Copenhagen, Copenhagen, Denmark. Correspondence: JB Andersen, MD, Department of Clinical Physiology, Nuclear Medicine and PET, Rigshospitalet, University of Copenhagen, Blegdamsvej 9, Copenhagen 2100, Denmark.
E-mail: Julie.bjerglund.andersen.01@regionh.dk
This work was supported in part by The Ludvig and Sara Elsass Foundation and Rigshospitalet, University of Copenhagen, Denmark. The hybrid PET/MR system at Rigshospitalet was donated by the John and Birthe Meyer Foundation.
Received 6 February 2015; revised 15 May 2015; accepted 18 May 2015; published online 10 June 2015

Experiments) guidelines. All procedures were performed under general anesthesia and all precautions were taken to minimize suffering.

## Animal Model

Seven healthy female newborn piglets (Danish landrace, mean weight 4.6 kg ± 0.2 s.d., mean age 3.4 weeks ± 0.4 s.d.) were delivered from a local farmer and scanned the same day. The piglets were anesthetized with an intramuscular injection of Zoletil (xylazine 2 mg/kg, ketamine 10 mg/kg, metadone 1 mg/kg, and butorphanol 1 mg/kg. Virbac, Denmark), hereafter tracheotomized and intubated. Spontaneous respiration was sufficient during the preparation and animals were kept in analgesia and anesthesia with intravenous fentanyl 10 $\mu$g/kg per hour and intravenous propofol 15 mg/kg per hour. Polyurethane catheters were placed in ear veins and subcutaneous abdominal veins bilaterally and in femoral arteries bilaterally. In total, four venous and two arterial catheters were placed and flushed with heparinized saline. For septic prophylaxis, ampicillin intravenous 200 mg/kg and gentamicin intravenous 4 mg/kg were administered as bolus injections. Fluid and glucose losses were compensated with intravenous isotonic glucose 20 mL/kg per hour.

When stable, the piglets were transported to the PET center covered in blankets and monitored by a portable capnograph (Secma, Skævinge, Denmark). In the scanner room, anesthesia was continued by intravenous propofol (15 to 20 mg/kg per hour) using a pump (B Braun, Melsungen, Germany) and intravenous fentanyl (10 $\mu$g/kg per hour) dosed by hand. If necessary, some piglets also received intravenous Zoletil (xylazine 0.2 mg/kg, ketamine 1 mg/kg, metadone 0.1 mg/kg, and butorphanol 0.1 mg/kg). Piglets were ventilated by an MR-compatible respirator (Fabius MRI, Dräger, Lübeck, Germany) with 30 to 60% oxygen, tidal volume ~ 35 mL. The piglets were monitored with invasive mean arterial pressure, heart rate, electro cardiogram, and capillary saturation displayed on a monitor. Rectal temperature was measured at the start and at the end of the experiment by a mercury thermometer.

The PET/MR scans were performed on the Siemens Biograph mMR system (Siemens, Erlangen, Germany).[10] The piglets were placed supine in the scanner and fitted with blankets. The field of view covered brain, heart, and thorax until the level of the liver. Data were acquired in a single bed position of 25.8 cm axial field of view.

Eight PET/MR scans for each piglet were performed with simultaneous PET $^{15}$O-water and ASL MR. Four scans at baseline and four scans after intravenous acetazolamide (Diamox, Mercury Pharmaceuticals, Croydon, UK) 10 mg/kg were conducted to compare methods at a wide range of CBF values. An interval of minimum 20 minutes after injection was included to obtain a new steady state. Acetazolamide is a commonly used vasodilator in cerebral studies[11,12] and 10 mg/kg was sufficient to elicit cerebral arteriolar vasodilatation in piglets in a previous study.[13] The PET scans were performed using either 20 MBq or 100 MBq $^{15}$O-water (four of each). The order of 20 MBq or 100 MBq injections was balanced by a Latin squared design (ABBABAAB). Arterial blood samples (0.5 mL) were collected from the left femoral arterial catheter after each scan to a total of eight samples per piglet and analyzed for partial pressure of carbon dioxide, partial pressure of oxygen, and oxygen saturation ($PaCO_2$ and $PaO_2$ and $SaO_2$) (ABL80Flex, Radiometer, Brønshøj, Denmark). During baseline scans, respiratory rate was adjusted to keep $PaCO_2$ at a constant level at around 5.5 kPa and after administration of acetazolamide to keep $PaCO_2$ below approximately 8 kPa. At the end of the experiments, the piglets were euthanized with an overdose of intravenous pentobarbital 150 mg/kg.

## MR Image Acquisition and Processing

The piglets were imaged using a 16-channel mMR head-neck array coil, designed by the vendor specifically for the PET/MR system to minimize radiation damping. When stable, high resolution three-dimensional T1-weighted image (magnetization-prepared rapid acquisition gradient echo (MP-RAGE)) was performed for anatomic imaging with the following parameters: Matrix size = 256 × 256, slice thickness = 1 mm, echo time = 2.44 milliseconds, repetition time = 1,900 milliseconds, field of view = 250 mm, flip angle 9°.

Arterial spin labeling scans were started simultaneously with $^{15}$O-water injection and continued for 7 minutes. Planning of the sequence was done on the MP-RAGE. Pulsed ASL was performed with the standard Siemens protocol (PICORE-Q2TIPS) with the following parameters: Single-shot echo planar imaging readout and parallel imaging acceleration factor = 2, flip angle 90°, matrix size = 64 × 64, voxel size = 3 × 3 × 4 mm$^3$, echo time = 11 ms, repetition time = 2,500 milliseconds, $TI_1$ = 800 milliseconds, $TI_{1s}$ = 1,600 milliseconds, $TI_2$ = 1,800 milliseconds, field of view = 192 mm, bandwidth = 2,232 Hz/pixel, 14 slices with slice thickness of 4 mm. The labeling plane was placed across the neck and upper thorax of the piglet. A total of 164 measurements were carried out, 82 pairs of label-control images. After each ASL scan, proton density-weighted images were acquired with the following parameters: matrix size: 64 × 64, echo time = 11 milliseconds, repetition time = 10,000 milliseconds, slice thickness 4 mm.

Global CBF was quantified in FSL (FMRIB software library).[14,15] A whole-brain region was drawn as a volume of interest on the anatomic MP-RAGE. The control-labeled differences were calculated and used to compute the perfusion-weighted maps. The maps were normalized by the proton density images. Quantification of CBF was performed according to established consensus for pulsed ASL Q2TIPS sequence to yield quantitative values in parametric maps in mL/100 g per minute (ASL CBF):[16,17]

$$C_{\mathrm{ASL}} = \frac{6000 \cdot \lambda \cdot (SI_{\mathrm{control}} - SI_{\mathrm{label}}) \cdot e^{\frac{TI}{T_{1,\mathrm{blood}}}}}{2 \cdot \alpha \cdot TI_1 \cdot SI_{\mathrm{PD}}}, \quad (1)$$

where $C_{\mathrm{ASL}}$denotes CBF, $\lambda$ is the brain/blood partition coefficient (0.9 mL/g), $SI_{\mathrm{control}}$ and $SI_{\mathrm{label}}$ are the time-averaged signal intensities in the control and label images, respectively, $T_{1,\mathrm{blood}}$ is the longitudinal relaxation time of blood (1,650 milliseconds), $\alpha$ is the labeling efficiency (0.98), $SI_{\mathrm{PD}}$ is the signal intensity of the proton density image.

## PET Image Acquisition and Processing

Dynamic scans were started approximately 60 seconds before either 20 MBq or 100 MBq $^{15}$O-water was injected to the left femoral vein as a short bolus (2 to 4 mL). The catheter was flushed with 2 mL heparinized isotonic saline. Data were collected in list mode for 8 minutes, initiated 1 minute before injection. There was a minimum interval of 12 minutes between injections to allow for tracer decay.

Approximately 60 seconds before $^{15}$O-water injection, arterial blood sampling for the measurement of arterial input function (AIF) was initiated using an automatic MR-compatible blood sampling system (Swisstrace, Menzingen, Switzerland) measuring activity in the blood every second. A shunt was constructed from the right femoral artery returning the blood through the right abdominal vein catheter using a peristaltic pump (Ismatec, Oak Harbour, WA, USA) with a withdrawal rate of 3 mL/min. The arterial catheter tip reached into the iliac artery. The length of the arterial catheter was 100 cm with an inner diameter of 1.0 mm. The distance from the artery to the detector block was approximately 15 cm. For blood clotting prophylaxis, intravenous heparin 100 IE/kg (LEO Pharma, Ballerup, Denmark) was administered.

Standard MR-based attenuation maps ($MR\_AC_{DIXON}$) were derived using the vendor provided DIXON VIBE sequence.[18] $MR\_AC_{DIXON}$ attenuation maps were reconstructed on 192 × 126 × 128 matrices (2.6 × 2.6 × 3.1 mm$^3$ voxels). Corrections including lung delineation were done in the $MR\_AC_{DIXON}$ and hereafter, co-registered full-dose CT attenuation values replaced the $MR\_AC_{DIXON}$ inside the brain region. Details are specified in the Supplementary Information.

The PET images were reconstructed using OP-OSEM (four iterations, 21 subsets, 2 mm Gaussian post filtering) on 256 × 256 matrices (1.1 × 1.1 × 2.0 mm$^3$ voxels) into the resulting PET data set. The data were sorted in the following manner: 1 × 30 seconds, 20 × 3 seconds, 10 × 5 seconds, 11 × 10 seconds, 4 × 20 seconds, 1 × 150 seconds. The reconstructed images were corrected for randoms, dead time, and decay. Scatter correction was performed as a model based single scatter simulation for three-dimensional PET.[19]

All PET analysis was done in PMOD (PMOD technologies, Zürich, Switzerland). A whole-brain region was drawn as a volume of interest on the MP-RAGE. A one-tissue compartment model adapted to $^{15}$O-water PET studies was applied. $K_1$, $k_2$, and delay was fitted simultaneously by the method by Meyer.[20] The dispersion was not fitted; for PET-AIF, dispersion was set to 3 seconds, and for PET-IDIF, the dispersion was set to 0 seconds. The equation applied is as follows:

$$C_{\mathrm{PET}}(t) = \tau K_1 C_{\mathrm{a}}(t) + (1 - \tau k_2) K_1 e^{-k_2 t} \int_0^t C_{\mathrm{a}}(\tau) e^{-k_2 \tau} \mathrm{d}\tau, \quad (2)$$

where $C_{\mathrm{PET}}$ denotes brain tissue activity at time $t$ (counts per second/g), $K_1$ (CBF) denotes the unidirectional blood to brain $^{15}$O-water clearance (mL/100 g per minute), $k_2$ denotes efflux rate constant (1/minute), $C_{\mathrm{a}}$ denotes arterial input function (counts per second/mL), and $\tau$ denotes dispersion.


© 2015 ISCBFM

**Table 1.** Physiologic parameters at baseline and at acetazolamide stimulus

| | *MAP(mm Hg)* | *Heart rate (beats/minute)* | *SAT (%)* | *Temp (°C)* | *$PaCO_2$ (kPa)* | *$PaO_2$ (kPa)* | *Hct (%)* |
|---|---|---|---|---|---|---|---|
| Baseline | 71 (67; 75) | 94 (87; 100) | 96 (95; 97) | 38.8 (38.1; 39.4) | 5.4 (5.2; 5.9) | 40 (36; 44) | 21 (20; 23) |
| Acetazolamide | 64 (58; 69) | 107 (97; 115) | 97 (96; 98) | 38.6 (38; 39.1) | 7.5 (7.3; 7.8) | 40 (35; 44) | 22 (21; 23) |
| Difference | −7.1[a] (−11.2; −3.1) | 13.2[a] (1.9; 24.5) | 0.6 (−1; 2.2) | −0.2 (−0.9; 0.1) | 2.2[a] (1.6; 2.8) | −0.8 (−7; 5.4) | 1.4 (−0.5; 3.2) |

Hct, hematocrit; MAP, mean arterial pressure; $PaCO_2$, partial pressure of $CO_2$; $PaO_2$, partial pressure of $O_2$; SAT, capillary saturation. [a]Significant difference ($P < 0.05$) between states by a mixed linear model. Values are arithmetic mean (95% confidence intervals). $N = 7$.

**Table 2.** Mean global cerebral blood flow in mL/100 g per minute (95% confidence intervals), test–retest variability, and mean difference to positron emission tomography arterial input function

| | | *Baseline* | | | *Acetazolamide* | | |
|---|---|---|---|---|---|---|---|
| *CBF method* | *Injected activity (MBq)* | *CBF 95% CI (mL/100 g per minute)* | *Test–retest (%)* | *ΔPET AIF (%)* | *CBF 95% CI (mL/100 g per minute)* | *Test–retest (%)* | *ΔPET AIF (%)* |
| PET AIF | 100 | 27.6 (24.0; 31.7) | 7.7 | | 64.4 (55.3; 74.9) | 9.8 | |
| | 20 | 27.4 (23.5; 32.1) | 5.7 | | 64.0 (55.0; 74.5) | 8.9 | |
| ASL | 100 | 29.5 (23.7; 36.7) | 8.6 | 2.3 | 76.8 (60.9; 96.8) | 8.2 | 19.3[a] |
| | 20 | 24.7 (19.0; 32.1) | 18.8[b] | −11.3 | 80.7 (63.7; 102.2) | 11.7 | 27.3[a] |
| PET IDIF | 100 | 33.6 (29.6; 38.1) | 5.9 | 21.8[a] | 78.6 (69.5; 88.9) | 9.0 | 22.1[a] |
| | 20 | 34.0 (29.9; 38.8) | 12.4 | 22.1[a] | 73.7 (64.1; 84.7) | 10.7 | 15.1[a] |

AIF, arterial input function; ASL, arterial spin labeling; CI; confidence interval; IDIF, image-derived input function; PET, positron emission tomography. Global CBF values from seven healthy newborn piglets calculated as geometric means. Cerebral blood flow is given in mL/100 g per minute. Test–retest: absolute variability. ΔPET AIF: relative difference to PET AIF CBF. Missing values: one in PET AIF, six in ASL (four in baseline 100 MBq scans). [a]Significant difference ($P < 0.05$) between methods by mixed linear model test. [b]Excluding an outlier gives test–retest 11.9% for 20 MBq scans.

Only the first 3 minutes from bolus arrival to the brain were used for modeling.

Two different input functions were used for kinetic modeling. The first derived from the automatic blood sampling system, arterial input function (AIF). The measured blood activity was corrected for background activity and decay corrected to the start of the PET scan.

The second was an image-derived input function (IDIF) generated from the dynamic PET sequence. This approach has previously been described in human and animal studies.[21–23] For each piglet, a box volume of interest containing the left ventricle of the heart was placed on the MP-RAGE and projected to the PET. In this box volume of interest, segmentation of the 75 voxels with highest activity was done in the average of the three 3-second PET frames (three-dimensional Gaussian 5 mm filter) where most of the activity was in the left ventricle. On the MP-RAGE, the positioning of the 75 voxels was evaluated, ensuring that placement was in the center of the left ventricle at a distance of minimum 5 mm to the myocardium. The 75 voxels were then projected to the dynamic PET sequence to generate the time activity curve for the IDIF. Details are specified in the Supplementary Information.

### Statistical Analysis

Initial comparisons of PET and ASL methods were made in Bland–Altman plots. As variance was seen to increase with increasing values, a logarithmic transformation was applied to the data before analysis. To evaluate the overall differences between methods and the effects of acetazolamide stimulus and injected activity of 20 MBq or 100 MBq, a linear mixed model for repeated measurements with group dependent residual variances was applied. Estimated effect of acetazolamide and between-method biases were expressed as expected difference in percentage with 95% confidence intervals and test–retest variability for the three methods were reported as absolute variability calculated as follows:

$$\text{Test}-\text{Retest} = \frac{|\text{scan}_1 - \text{scan}_2|}{0.5(\text{scan}_1 + \text{scan}_2)},$$

where $\text{scan}_1$ and $\text{scan}_2$ refer to CBF estimates with the same injected activity (100 MBq or 20 MBq). Statistical significance was defined as $P < 0.05$. All analyses were performed with SAS version 9.3 (SAS Institute, Cary, NC, USA).

## RESULTS

The mean values for measured physiologic parameters during baseline and acetazolamide are shown in Table 1. Mean arterial pressure decreased significantly with 7.1 (95% CI: −11.2; −3.1) mm Hg and $PaCO_2$ increased significantly with 2.2 (1.6; 2.8) kPa. Heart rate increased significantly with 13.2 (1.9; 24.5) beats/minute. No significant changes were observed in capillary saturation, rectal temperature, $PaO_2$, or Hct (hematocrit).

Six ASL scans were not useful because of erroneous table position shifts (one in two piglets, two in two piglets), so a total of 56 PET scans and 50 ASL scans were successful. In the kinetic modeling, the mean PET AIF delay was 3.6 seconds (2.9; 4.3), and the mean PET IDIF delay was −1.9 seconds (−1.7; −2.1).

Positron emission tomography CBF using the arterial input function (PET AIF) and PET using the image-derived input function (PET IDIF) were at baseline 27 (23;32), 34 (31;37), and mL/100 g per minute, respectively, and the mean ASL CBF was 27 (22;32) mL/100 g per minute. At acetazolamide stimulus, PET AIF CBF and PET IDIF CBF were 64 (55;74), 76 (70;83) mL/100 g per minute, respectively, and the mean ASL CBF were 79 (67;92) mL/100 g per minute. Mixed linear analysis estimated the effect of acetazolamide as an increase in median PET AIF CBF by a factor 2.3 (2;2.7). There was a significant effect of acetazolamide on CBF bias between methods with statistically significant bias between PET AIF and ASL ($P = 0.0003$) and PET AIF and PET IDIF ($P = 0.0008$). At baseline, a significant difference was found between PET AIF and PET IDIF ($P < 0.0001$). In comparison with PET AIF, ASL underestimated CBF slightly at baseline (−0.7% mean difference) and overestimated CBF at acetazolamide stimulus (23.6% mean difference). PET IDIF overestimated CBF at both baseline and acetazolamide stimulus (21.9% and 18.9%, respectively). There was a significant difference in variances between methods when accounting for dose and acetazolamide effect ($P = 0.01$). Arterial spin labeling showed the largest variance, and PET AIF showed the smallest variance.

© 2015 ISCBFM

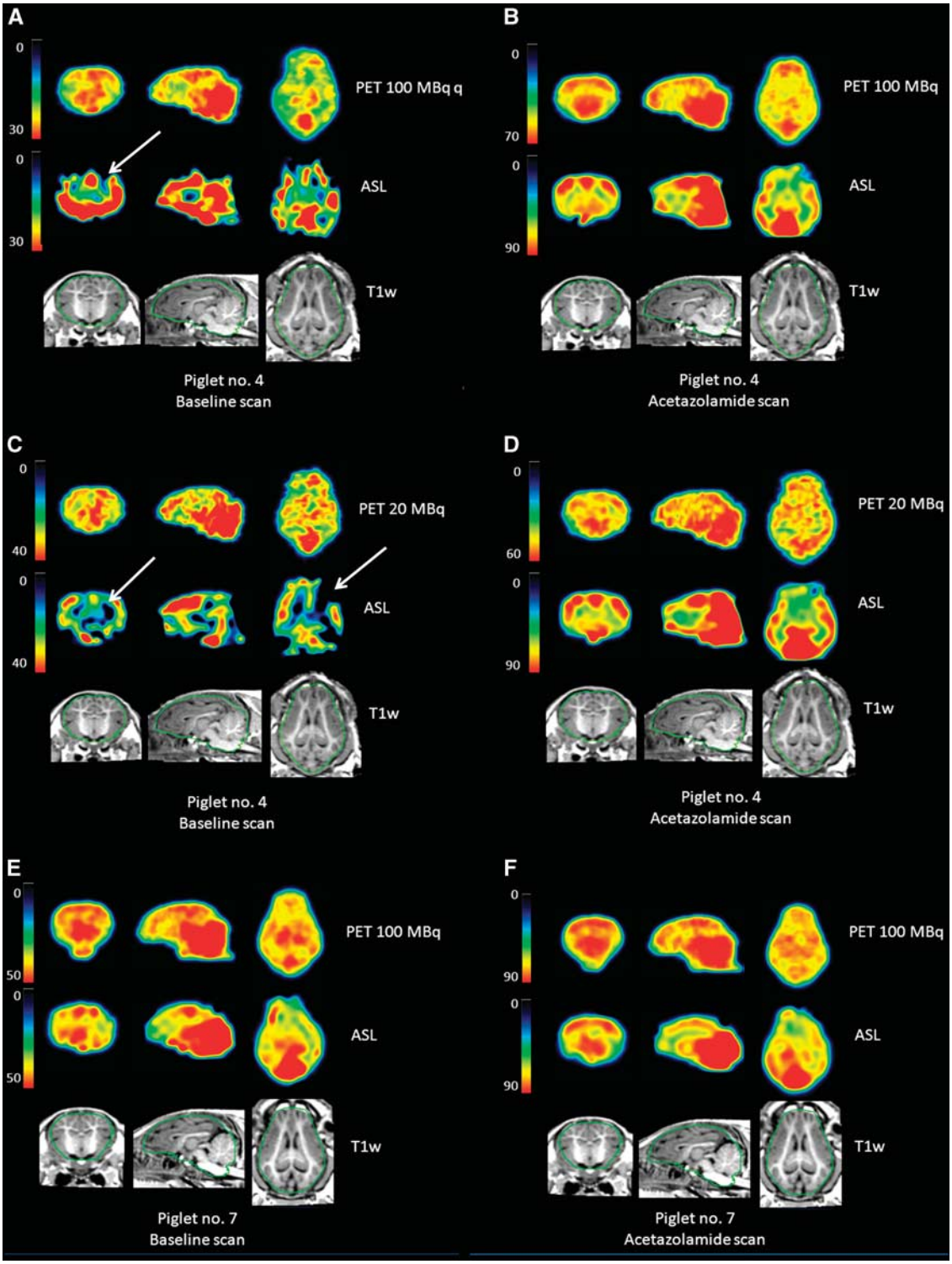


**Figure 1.** Regional CBF images for two piglets: Co-registered slices through the level of the basal ganglia showing anatomic MP-RAGE, regional CBF images from PET AIF and ASL, shown in 5 mm Gaussian filtering. Images quantified in mL/100 g per minute. The PET CBF images were calculated using the PMOD implementation of Alperts[47] time-weighted integral method for dynamic data with dispersion fixed at 3 seconds and delay fitted by the method of Meyer.[20] (**A**) Piglet no. 4 baseline scan showing PET 100 MBq scan (top), ASL (middle), and MP-RAGE (bottom). (**B**) Piglet no. 4 acetazolamide scan showing PET 100 MBq scan (top), ASL (middle), and MP-RAGE (bottom). (**C**) Piglet no. 4 baseline scan showing 3 mm PET 20 MBq scan (top), ASL (middle), and MP-RAGE (bottom). (**D**) Piglet no. 4 acetazolamide scan showing PET 20 MBq scan (top), ASL (middle), and MP-RAGE (bottom). (**E**) Piglet no. 7 baseline scan showing PET 100 MBq scan (top), ASL (middle), and MP-RAGE (bottom). (**F**) Piglet no. 7 acetazolamide scan showing PET 100 MBq scan (top), ASL (middle) and MP-RAGE (bottom). A high level of noise is represented in ASL CBF images, exemplified by negative value voxels in **A** and **C** (white arrows), even at 5 mm Gaussian filtering. The 20 MBq PET CBF image (**C** and **D**) display a larger degree of noise compared with 100 MBq PET CBF image (**A** and **B**). AIF, arterial input function; ASL, arterial spin labeling; MP-RAGE, magnetization-prepared rapid acquisition gradient echo; PET, positron emission tomography.


© 2015 ISCBFM

Table 2 shows the results of the global CBF for ASL, PET AIF, and PET IDIF. Values for injected activity (100 MBq and 20 MBq) are shown. Using a tracer activity of 20 MBq resulted in a higher variance when assuming no acetazolamide effect ($P = 0.06$) and when accounting for acetazolamide effect ($P = 0.08$), but the differences were not significant. Test–retest variability was similar for 100 MBq injected activity for the three methods (ASL 8.2%, PET IDIF 7.5%, and PET AIF 8.6%). Test–retest variability for 20 MBq for PET IDIF was higher than PET AIF (11.6% versus 7.4%). Test–retest variability for ASL was higher in the 20 MBq PET scan sessions (15.9%), however, when excluding an outlier with a high variability of over 60%, test–retest was 11.9%.

Cerebral blood flow images for PET and ASL along with anatomic MP-RAGE as reference for two piglets are shown in Figure 1. Both modalities showed a similar perfusion pattern with higher perfusion in the cerebellum and occipital lobes, however, the ASL CBF image showed higher perfusion values in these areas than PET CBF image. This pattern was represented in all the other piglets. It was also seen that the variation across voxels was greater in ASL than PET images, with more voxels with very low and very high values as seen in Figure 1A. Piglet no. 4 showed a greater tendency for low value voxels than piglet no. 7. Voxels with negative values were observed in deep white matter but also in frontal and parietal cortex as shown in Figures 1A and 1C of piglet no. 4. In this piglet, negative value voxels were most prominent, while it was less prominent in other piglets as seen in Figure 1E of piglet no. 7. Notice also the high perfusion values at the base of the brain in the ASL CBF image in Figures 1A, 1C and 1E, all in baseline scans, representing high signal intensity near the temporal lobes. This was in contrast to the PET CBF image. The 20 MBq PET CBF images displayed a larger regional noise level (Figures 1C and 1D, ) but with a similar tracer distribution.

Higher bias at higher CBF values were observed on a scatter plot of global CBF values, as shown in Figure 2A. On a logarithmic scale, the plot was more uniform (Figure 2B) indicating a relative bias between the two CBF methods. By tracking the values of each piglet (Figures 2A and 2B), it was shown that acetazolamide scans had a wider variance in ASL CBF values than PET CBF values. One piglet had lower ASL CBF values at acetazolamide than PET, which was in contrast to the trend of ASL CBF overestimation at higher CBF values.

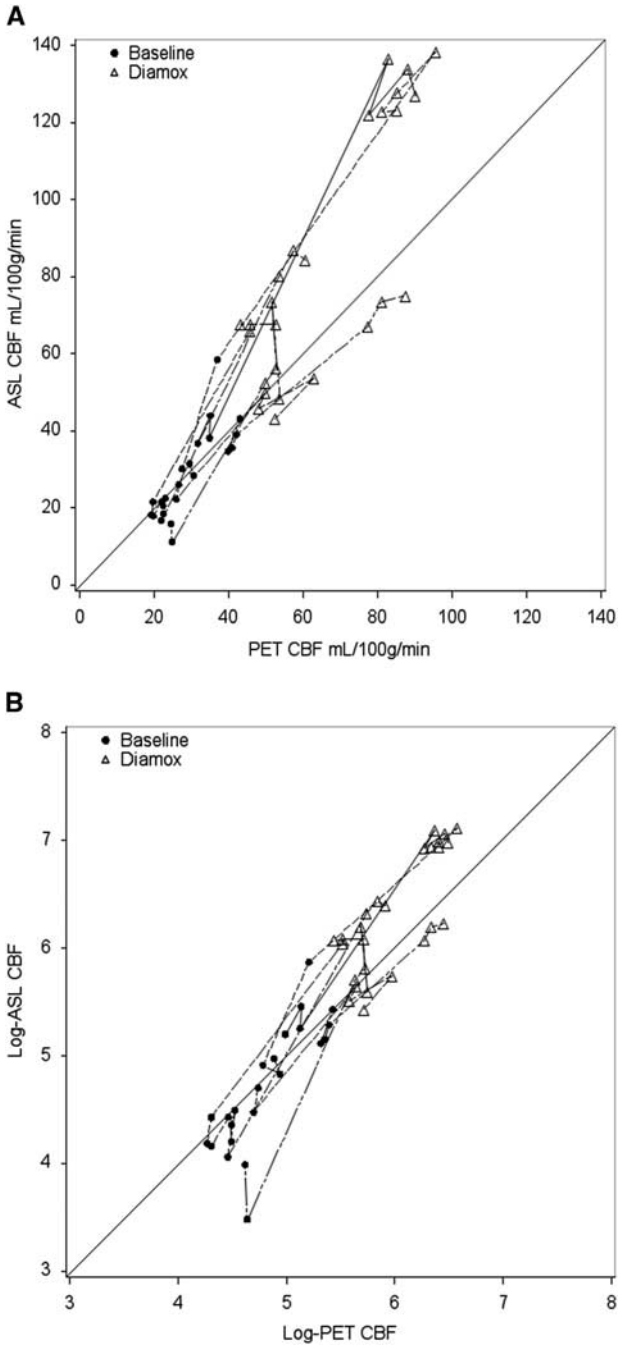


**Figure 2.** Scatter plots of PET CBF and ASL CBF values. Scatter plot of the same data plotted by (**A**) global PET CBF by arterial input function (AIF) and global ASL CBF in mL/100 g per minute; baseline scans (dots) and acetazolamide scans (triangles). Tracking of seven individual piglets with different line types; line of identity (full line). (**B**) Logarithmic transformation of PET AIF CBF and ASL CBF; baseline scans (dots) and acetazolamide scans (triangles). Tracking of seven individual piglets in different line types; line of identity (full line). By logarithmic transformation, the distribution of CBF values along the line of identity was more even. ASL, arterial spin labeling; PET, positron emission tomography.

## DISCUSSION

We have simultaneously investigated two quantitative methods for the estimation of global CBF in a newborn piglet model on our PET/MR hybrid scanner with the aim of developing a clinical method for CBF measurements in newborn infants. Positron emission tomography was performed with injected activity of both 100 MBq and 20 MBq $^{15}$O-water. This was done to study any adverse effects on CBF quantification of an injected activity level low enough to be acceptable for non-therapeutic research use in newborn infants. The injected activity of $^{15}$O-water given to the piglets was 4.3 MBq/kg or 0.33 mSv ionizing radiation dose, which corresponds to approximately 1 month background radiation for a healthy person in Denmark.

Our study demonstrated that global CBF in newborn piglets using ASL and PET were congruent during baseline conditions but not during acetazolamide stimulus. Baseline ASL scans showed a large variation in voxel values including very high values and negative values. A systematic overestimation of global PET CBF was found when using IDIF. PET CBF performed with 20 MBq showed acceptable concordance with PET CBF performed with 100 MBq. Thus 20 MBq may be used clinically without compromising image quality significantly. The PET IDIF CBF showed an overestimation of approximately 20%. This would be an unacceptable result for comparison of clinical methods, especially if the difference was heterogenic with a high variance. In future research, it should be validated that a shorter time frame, e.g., 1 or 2 seconds, would limit the overestimation further. However, a short time frame would also contribute with noise especially in very low activity scans using 20 MBq. If a shorter time framing could not be possible, future studies deriving the IDIF from the heart in PET $^{15}$O-water studies,

© 2015 ISCBFM

should be aware of the possible overestimation of CBF values. Another source of bias to the IDIF was the possible contamination of myocardial uptake because of cardiac wall movements. This would be manifest as an increasing IDIF tail, which was not seen.

The reduction of injected activity to 20 MBq increased the variance and test–retest variability of CBF compared with 100 MBq (Table 2), although not significantly. This is expected and a consequence of the increase in Poisson noise. It may introduce a bias in reconstruction as previously shown.[24,25] However, we found that the increased regional noise level in PET images was at an acceptable level to qualify the application in newborn children to quantify regional CBF, not least, as the brain volume is substantially larger than in piglets. Pulsed ASL has inherent low SNR. The review of CBF images revealed large variations in ASL CBF images at the voxel level especially in low CBF areas, compared with the PET CBF images. Voxel values were in some piglets zero or below indicating inaccuracy. A high proportion of negative voxels has been reported in newborn infants with cardiac malformations and low CBF, and omitting the negative voxels from the estimation of global CBF was suggested.[26] Our data suggest that this procedure would increase the positive bias of ASL compared with PET.

In our study, we made use of a single post-labeling delay of 1,000 milliseconds (TI-$TI_1$) using the PICORE sequence which could partly explain the large variation at voxel level in ASL images, since the PICORE sequence using a single TI most likely does not fit all piglets because of the variation of arterial transit time in tissues between piglets and between physiologic state. A short delay increased the likelihood of incomplete delivery of labeled blood to the tissue. However, arterial transit time, e.g., the time from label of blood to arrival in capillary bed, has been estimated to 630 milliseconds in piglets[27] but up to ~1,000 milliseconds in premature infants.[28] Arterial transit time can vary across brain regions with longest time in water-shed areas between vascular territories and in white matter.[29] Setting a suitable delay is a tradeoff between sufficient delivery of tracer to the tissue and decreased SNR because of decay of blood spins ($T_{1,blood}$). A multi-TI approach to estimate regional arterial transit time and fitting of data could increase the accuracy of CBF estimates in regions with longer arterial transit time, e.g., white matter.[30] This could limit the risk of very low value voxels, which with a single T1 approach may not specifically reflect a low CBF value but rather a low signal. In pulsed ASL, the large tagging area used on the piglets, may also have given rise to cross-contamination of systemic tagged blood as previously suggested.[26] This may also have contributed to the large variation in voxel values in ASL CBF images.

Further, subject-specific estimates of ASL parameters, particularly $T_{1,blood}$ and $T_{1,tissue}$ could improve the accuracy of CBF measurements[28] to account for minor differences between subjects. In our study, we have used parameters derived from internationally recognized recommendations to the clinical implementation of the pulsed ASL sequence regarding $T_{1,blood}$ and labeling efficiency ($\alpha$).[16] The recommended $T_{1,blood}$ value is derived from bovine blood,[31] which we assume to be similar to pig blood. Separate pig $T_{1,blood}$ has not been reported in the literature. Koziak *et al*[27] found $T_{1,tissue}$ in newborn piglets in gray and white matter at 3 T to be 1,646 ± 50 milliseconds and 1,368 ± 44 milliseconds, respectively. The gray matter $T_{1,tissue}$ is relatively similar to human gray matter found at 1,608 milliseconds at 3 T.[32] Thus, a value of 1,650 milliseconds is appropriate for $T_{1,blood}$ and the difference to gray matter $T_{1,tissue}$ in piglets is relatively small.

The ASL sequence can influence CBF accuracy. Arterial spin labeling has been considered unsuitable to quantify white matter CBF,[29] but recent technical advances may change this circumstance.[33] Pseudo-continuous ASL (pCASL) is recommended for clinical imaging[16] and contributes with an improvement in SNR also in high-risk neonates[34] in comparison with pulsed ASL. Because of limitations in the software platform, pCASL was not available on our PET/MR system at the time of the study. However, for future research, our piglet model for simultaneous PET CBF and ASL CBF on a hybrid PET/MR has been proposed and validated. In future projects, the use of optimized ASL sequences using multi-TI and three-dimensional readout for improved SNR should be applied. The possibilities for comparison between other PET tracers using the heart IDIF and ASL for CBF imaging is promising for studies of neonatal hypoxic–ischemic brain damage. Regarding ASL in newborn infants, further research will be necessary to test ASL CBF regional accuracy in white matter, which is clinically the most important brain area when quantifying CBF in newborn infants suspected of hypoxic–ischemic brain damage.

Our study suggests that ASL may be used to measure global CBF in newborn infants in baseline conditions. However, when using a pulsed single TI ASL approach, negative value voxels in CBF images, higher variance and higher test–retest variability for global ASL CBF were seen. Arterial spin labeling CBF results should be used critically since newborn infants have inherently low CBF that challenges the ASL method. Preferably, subject-specific parameters should be used when feasible.[28,35] As ASL provides one-shot static CBF, it is not useful for monitoring but can be performed as an add-on when conventional MR and MR spectroscopy are performed. It is clinically relevant to measure absolute CBF values in newborn infants, and global CBF in neonates is only one-third of adult CBF.[36–38] Premature infants are at a risk of developing hypoxic–ischemic damage as well as intracerebral hemorrhage at low CBF values[36,37] and monitoring of cerebral hemodynamics is an important tool in caring for premature and sick infants.[1,7] Previous neonatal CBF studies using single photon emission computed tomography have shown a very low CBF in white matter of premature infants, but the method was limited by corrections and partial volume effects.[2,3] Older PET studies were limited by a low spatial resolution.[36–38] Positron emission tomography and single photon emission computed tomography both give ionizing radiation, which limit applications. Arterial spin labeling being noninvasive and radiation free, has been used in studies in newborn infants when absolute regional CBF values were investigated.[4–6,28,39,40] However, no validation studies on neonatal ASL CBF have been conducted, a few human studies compare ASL and PET CBF in adults[41–44] and only one on a hybrid PET/MR system.[45] Few piglet studies on ASL and PET CBF have been conducted.[27,46]

The advantage of our study is the simultaneous measurements of CBF with PET and ASL. However, the study has limitations. Our investigations serve as a pilot study to investigate the potentials of the hybrid PET/MR system for imaging in newborn infants; therefore the sample size was small. The piglet model only allowed investigation of global CBF values as the white matter regions in the newborn piglet were too narrow (3 to 4 mm) for reliable estimation of white matter CBF when the best obtainable resolution in PET was 4 mm and in ASL 3 mm.

In conclusion, minimally invasive PET approaches with low injected activity of $^{15}$O-water and noninvasive image-derived input function was possible for quantification of CBF in newborn piglets. However, an overestimation of approximately 20% was observed using an IDIF and further validation is needed. Arterial spin labeling global CBF in newborn piglets were congruent with PET CBF during baseline conditions but not during acetazolamide stimulus, questioning global ASL CBF precision and reliability. Single TI ASL does not seem suitable for regional CBF measurements in newborn infants. Clinical studies to compare PET and ASL CBF in newborn infants on a hybrid PET/MR system using optimized ASL and multi-TI approach await further evaluation.


© 2015 ISCBFM

## AUTHOR CONTRIBUTIONS

JBA contributed with design, acquisition, analysis and interpretation of data, drafting and revising the manuscript, and final approval of the manuscript. WH contributed with acquisition of data, revising and approving the manuscript, UL contributed with design and analysis of data, revising and approving the manuscript, CNL contributed with design and analysis of data, revising and approving the manuscript, LH contributed with design and interpretation, revising and approving the manuscript, GG contributed with design and interpretation of data, revising and approving the manuscript, IL contributed with design, analysis and interpretation of data, revising and approving the manuscript.

## DISCLOSURE/CONFLICT OF INTEREST

The authors declare no conflict of interest.

## ACKNOWLEDGMENTS

The authors thank Nuclear Medicine Technologists Marianne Federspiel, Karin Stahr, and Radiographer Jakup Madsen at the Department of Clinical Physiology, Nuclear Medicine and PET, and Veterinary Assistant Mette Værum Olesen at the Department of Experimental Medicine, University of Copenhagen for their valuable assistance in the studies. The authors also thank the Cyclotron Unit at the Department of Clinical Physiology, Nuclear Medicine and PET for reliable delivery of $^{15}$O-water, and Associate Professor Julie Lyng Forman at Section for Biostatistics, Department of Public Health, University of Copenhagen for assistance with the statistics.

## REFERENCES

1 du Plessis AJ. Cerebrovascular injury in premature infants: current understanding and challenges for future prevention. *Clin Perinatol* 2008; **35**: 609–641.
2 Borch K, Greisen G. Blood flow distribution in the normal human preterm brain. *Pediatr Res* 1998; **43**: 28–33.
3 Borch K, Lou HC, Greisen G. Cerebral white matter blood flow and arterial blood pressure in preterm infants. *Acta Paediatr* 2010; **99**: 1489–1492.
4 Massaro AN, Bouyssi-Kobar M, Chang T, Vezina LG, du Plessis AJ, Limperopoulos C. Brain perfusion in encephalopathic newborns after therapeutic hypothermia. *AJNR Am J Neuroradiol* 2013; **34**: 1649–1655.
5 Wintermark P, Hansen A, Gregas MC, Soul J, Labrecque M, Robertson RL *et al.* Brain perfusion in asphyxiated newborns treated with therapeutic hypothermia. *AJNR Am J Neuroradiol* 2011; **32**: 2023–2029.
6 De Vis JB, Hendrikse J, Petersen ET, de Vries LS, van BF, Alderliesten T *et al.* Arterial spin-labelling perfusion MRI and outcome in neonates with hypoxic-ischemic encephalopathy. *Eur Radiol* 2015; **25**: 113–121.
7 Liem KD, Greisen G. Monitoring of cerebral haemodynamics in newborn infants. *Early Hum Dev* 2010; **86**: 155–158.
8 Herscovitch P, Markham J, Raichle ME. Brain blood flow measured with intravenous H2O. I. Theory and error analysis. *J Nucl Med* 1983; **24**: 782–789.
9 Raichle ME, Martin WR, Herscovitch P, Mintun MA, Markham J. Brain blood flow measured with intravenous H2(15)O. II. Implementation and validation. *J Nucl Med* 1983; **24**: 790–798.
10 Delso G, Furst S, Jakoby B, Ladebeck R, Ganter C, Nekolla SG *et al.* Performance measurements of the Siemens mMR integrated whole-body PET/MR scanner. *J Nucl Med* 2011; **52**: 1914–1922.
11 Lassen NA, Friberg L, Kastrup J, Rizzi D, Jensen JJ. Effects of acetazolamide on cerebral blood flow and brain tissue oxygenation. *Postgrad Med J* 1987; **63**: 185–187.
12 Vorstrup S, Henriksen L, Paulson OB. Effect of acetazolamide on cerebral blood flow and cerebral metabolic rate for oxygen. *J Clin Invest* 1984; **74**: 1634–1639.
13 Domoki F, Zimmermann A, Toth-Szuki V, Busija DW, Bari F. Acetazolamide induces indomethacin and ischaemia-sensitive pial arteriolar vasodilation in the piglet. *Acta Paediatr* 2008; **97**: 280–284.
14 Chappell MA, Groves AR, Whitcher B, Woolrich MW. Variational Bayesian Inference for a Nonlinear Forward Model. *IEEE Trans Signal Process* 2009; **57**: 223–236.
15 Jenkinson M, Beckmann CF, Behrens TE, Woolrich MW, Smith SM. FSL. *Neuroimage* 2012; **62**: 782–790.
16 Alsop DC, Detre JA, Golay X, Gunther M, Hendrikse J, Hernandez-Garcia L *et al.* Recommended implementation of arterial spin-labeled perfusion MRI for clinical applications: a consensus of the ISMRM perfusion study group and the European consortium for ASL in dementia. *Magn Reson Med* 2014; **73**: 102–116.
17 Wong EC, Buxton RB, Frank LR. Quantitative imaging of perfusion using a single subtraction (QUIPSS and QUIPSS II). *Magn Reson Med* 1998; **39**: 702–708.
18 Martinez-Moller A, Souvatzoglou M, Delso G, Bundschuh RA, Chefd'hotel C, Ziegler SI *et al.* Tissue classification as a potential approach for attenuation correction in whole-body PET/MRI: evaluation with PET/CT data. *J Nucl Med* 2009; **50**: 520–526.
19 Watson CC. New, faster, image-based scatter correction for 3D PET. *IEEE Trans Nucl Sci* 2000; **47**: 1587–1594.
20 Meyer E. Simultaneous correction for tracer arrival delay and dispersion in CBF measurements by the H215O autoradiographic method and dynamic PET. *J Nucl Med* 1989; **30**: 1069–1078.
21 Kim J, Herrero P, Sharp T, Laforest R, Rowland DJ, Tai YC *et al.* Minimally invasive method of determining blood input function from PET images in rodents. *J Nucl Med* 2006; **47**: 330–336.
22 Baudrexel S, Graf R, Knoess C, Vollmar S, Wienhard K. Derivation of the input function from dynamic PET Images with the HRRT. *IEEE Nucl Sci Symp Conf Rec* 2004; **6**: 3890–3892.
23 Iida H, Miura S, Shoji Y, Ogawa T, Kado H, Narita Y *et al.* Noninvasive quantitation of cerebral blood flow using oxygen-15-water and a dual-PET system. *J Nucl Med* 1998; **39**: 1789–1798.
24 Jian Y, Planeta B, Carson RE. Evaluation of bias and variance in low-count OSEM list mode reconstruction. *Phys Med Biol* 2015; **60**: 15–29.
25 Cheng JC, Blinder S, Rahmim A, Sossi V. A scatter calibration technique for dynamic brain imaging in high resolution PET. *IEEE Trans Nucl sci* 2010; **57**: 225–233.
26 Wang J, Licht DJ, Silvestre DW, Detre JA. Why perfusion in neonates with congenital heart defects is negative--technical issues related to pulsed arterial spin labeling. *Magn Reson Imaging* 2006; **24**: 249–254.
27 Koziak AM, Winter J, Lee TY, Thompson RT, St, Lawrence KS. Validation study of a pulsed arterial spin labeling technique by comparison to perfusion computed tomography. *Magn Reson Imaging* 2008; **26**: 543–553.
28 Varela M, Petersen ET, Golay X, Hajnal JV. Cerebral blood flow measurements in infants using look-locker arterial spin labeling. *J Magn Reson Imaging* 2014; **41**: 1591–1600.
29 van Gelderen P, de Zwart JA, Duyn JH. Pittfalls of MRI measurement of white matter perfusion based on arterial spin labeling. *Magn Reson Med* 2008; **59**: 788–795.
30 Qiu D, Straka M, Zun Z, Bammer R, Moseley ME, Zaharchuk G. CBF measurements using multidelay pseudocontinuous and velocity-selective arterial spin labeling in patients with long arterial transit delays: comparison with xenon CT CBF. *J Magn Reson Imaging* 2012; **36**: 110–119.
31 Lu H, Clingman C, Golay X, van Zijl PC. Determining the longitudinal relaxation time (T1) of blood at 3.0 Tesla. *Magn Reson Med* 2004; **52**: 679–682.
32 Wright PJ, Mougin OE, Totman JJ, Peters AM, Brookes MJ, Coxon R *et al.* Water proton T1 measurements in brain tissue at 7, 3, and 1.5 T using IR-EPI, IR-TSE, and MPRAGE: results and optimization. *MAGMA* 2008; **21**: 121–130.
33 Mutsaerts HJ, Richard E, Heijtel DF, van Osch MJ, Majoie CB, Nederveen AJ. Gray matter contamination in arterial spin labeling white matter perfusion measurements in patients with dementia. *Neuroimage Clin* 2014; **4**: 139–144.
34 Goff DA, Buckley EM, Durduran T, Wang J, Licht DJ. Noninvasive cerebral perfusion imaging in high-risk neonates. *Semin Perinatol* 2010; **34**: 46–56.
35 De Vis JB, Hendrikse J, Groenendaal F, de Vries LS, Kersbergen KJ, Benders MJ *et al.* Impact of neonate haematocrit variability on the longitudinal relaxation time of blood: Implications for arterial spin labelling MRI. *Neuroimage Clin* 2014; **4**: 517–525.
36 Lou HC, Lassen NA, Friis-Hansen B. Impaired autoregulation of cerebral blood flow in the distressed newborn infant. *J Pediatr* 1979; **94**: 118–121.
37 Milligan DW. Failure of autoregulation and intraventricular haemorrhage in preterm infants. *Lancet* 1980; **1**: 896–898.
38 Volpe JJ, Herscovitch P, Perlman JM, Raichle ME. Positron emission tomography in the newborn: extensive impairment of regional cerebral blood flow with intraventricular hemorrhage and hemorrhagic intracerebral involvement. *Pediatrics* 1983; **72**: 589–601.
39 De Vis JB, Petersen ET, de Vries LS, Groenendaal F, Kersbergen KJ, Alderliesten T *et al.* Regional changes in brain perfusion during brain maturation measured non-invasively with Arterial Spin Labeling MRI in neonates. *Eur J Radiol* 2013; **82**: 538–543.
40 Duncan AF, Caprihan A, Montague EQ, Lowe J, Schrader R, Phillips JP. Regional Cerebral Blood Flow in Children From 3 to 5 Months of Age. *AJNR Am J Neuroradiol* 2013; **35**: 593–598.
41 Arbelaez AM, Su Y, Thomas JB, Hauch AC, Hershey T, Ances BM. Comparison of regional cerebral blood flow responses to hypoglycemia using pulsed arterial spin labeling and positron emission tomography. *PLoS One* 2013; **8**: e60085.
42 Heijtel DF, Mutsaerts HJ, Bakker E, Schober P, Stevens MF, Petersen ET *et al.* Accuracy and precision of pseudo-continuous arterial spin labeling perfusion

© 2015 ISCBFM

during baseline and hypercapnia: a head-to-head comparison with (1)(5)O H(2)O positron emission tomography. *Neuroimage* 2014; **92**: 182–192.

43 van Golen LW, Kuijer JP, Huisman MC, IJzerman RG, Barkhof F, Diamant M *et al*. Quantification of cerebral blood flow in healthy volunteers and type 1 diabetic patients: comparison of MRI arterial spin labeling and [(15)O] H2O positron emission tomography (PET). *J Magn Reson Imaging* 2014; **40**: 1300–1309.

44 Henriksen OM, Larsson HB, Hansen AE, Gruner JM, Law I, Rostrup E. Estimation of intersubject variability of cerebral blood flow measurements using MRI and positron emission tomography. *J Magn Reson Imaging* 2012; **35**: 1290–1299.

45 Zhang K, Herzog H, Mauler J, Filss C, Okell TW, Kops ER *et al*. Comparison of cerebral blood flow acquired by simultaneous [15O]water positron emission tomography and arterial spin labeling magnetic resonance imaging. *J Cereb Blood Flow Metab* 2014; **34**: 1373–1380.

46 Mortberg E, Cumming P, Wiklund L, Wall A, Rubertsson S A. PET study of regional cerebral blood flow after experimental cardiopulmonary resuscitation. *Resuscitation* 2007; **75**: 98–104.

47 Alpert NM, Eriksson L, Chang JY, Bergstrom M, Litton JE, Correia JA *et al*. Strategy for the measurement of regional cerebral blood flow using short-lived tracers and emission tomography. *J Cerebr Blood Flow Metab* 1984; **4**: 28–34.

This work is licensed under a Creative Commons Attribution-NonCommercial-NoDerivs 4.0 International License. The images or other third party material in this article are included in the article's Creative Commons license, unless indicated otherwise in the credit line; if the material is not included under the Creative Commons license, users will need to obtain permission from the license holder to reproduce the material. To view a copy of this license, visit http://creativecommons.org/licenses/by-nc-nd/4.0/

Supplementary Information accompanies the paper on the Journal of Cerebral Blood Flow & Metabolism website (http://www.nature.com/jcbfm)


© 2015 ISCBFM